ELSEVIER

Polymer 42 (2001) 4353–4366

polymer

www.elsevier.nl/locate/polymer

Small angle light scattering investigation of polymerisation induced phase separation mechanisms

J. Maugey, T. Van Nuland, P. Navard*

Ecole des Mines de Paris, Centre de Mise en Forme des Matériaux (CEMEF), UMR CNRS 7635, BP 207, 06904 Sophia-Antipolis Cedex, France

Received 15 May 2000; received in revised form 13 September 2000; accepted 10 October 2000

Abstract

Small angle light scattering (SALS) is one of the tools that can be used to study a phase separation. It is shown that SALS can be used to discriminate between nucleation and growth (NG) and spinodal decomposition (SD) even when both give a pattern composed of a ring. To support this, a complete calculation of the light scattering of an NG process is performed, taken into account the correct Mie form factor and adding polydispersity, multiple scattering and non-independent scattering. All these factors are shown to play a role that gives patterns that cannot be confused with the one originating from an SD. © 2001 Elsevier Science Ltd. All rights reserved.

Keywords: Nucleation–growth; Spinodal decomposition; Light-scattering

1. Introduction

The separation of a homogeneous mixture into two phases can proceed through two main ways, spinodal decomposition (SD) and nucleation and growth (NG) [1–3]. The selection of the mechanism will depend on the thermodynamic balance between the two components and is mainly driven by the quench depth and the composition. These two processes are different and produce very different morphologies. SD gives a 3D space interconnected region of phase A-rich and phase B-rich areas. It takes place if the mixture is quenched into an unstable zone of the phase diagram. The growth originates from a small and periodic fluctuation of composition. The behaviour of the mean distance between the regions and the increase in concentration of the major component in their respected phases are well documented [4,5]. In some cases the high surface energy represented by the co-continuous structure will induce a structure break-up with or without coalescence. Coming from an SD, the resulting droplets will be regularly dispersed and the particle size will be quite uniform.

On the other hand, NG produces a very different morphology [6–8]. It starts with the random building of nuclei with a size above a critical one. Most of the time, these nuclei will grow with the same growth rate in all directions (in isotropic fluids). The morphology is thus composed of spheres of phase A-rich regions in a phase B-rich continuous matrix. In the early stages of the NG process, it is easy to obtain a rate equation for the radius of the sphere by solving the diffusion equation [2]:

$$\frac{\mathrm{d}R}{\mathrm{d}t} = \frac{D}{R}\left[\Delta - \frac{\alpha}{R}\right] \tag{1}$$

(this means $R \propto t^{1/2}$ if α is small). D is the diffusion coefficient, Δ the relative supersaturation and α the interface thickness.

In the late stages of growth, Lifishitz and Slyozov [9] calculated the behaviour of the droplet radius distribution function and showed that the mean radius of the spheres obeys the following law:

$$\bar{R} \propto t^{1/3} \tag{2}$$

In the late stage (coarsening process), larger droplets grow at the expense of smaller droplets. This results from an evaporation–condensation mechanism in which the atoms of the minority phase diffuse to the matrix from smaller droplets that are dissolving to larger droplets that are growing. This behaviour is also called Ostwald ripening.

In both cases, since the system will be transformed from a homogeneous mixture with a single refractive index to a mixture with two distinct phases (thus with two different refractive indexes), small angle light scattering (SALS) is the obvious, most simple tool to study such phase separations in the type of systems under consideration here [10–15]. SALS is determined by two factors: one resulting

* Corresponding author. Tel.: +33-4-93-95-74-66; fax: +33-4-92-38-97-52.

E-mail address: patrick.navard@cemef.cma.fr (P. Navard).

PII: S0032-3861(00)00743-6

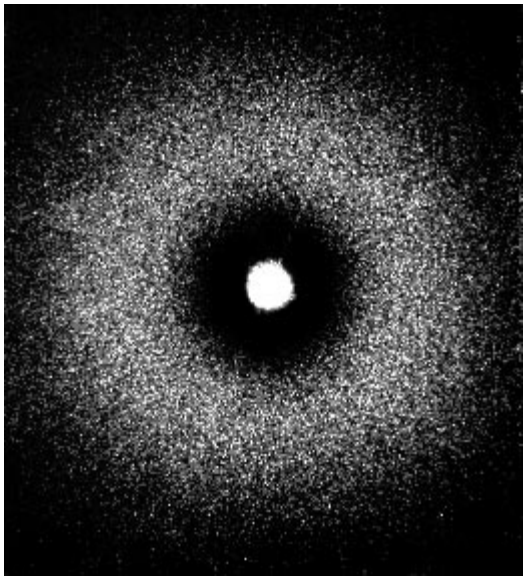

Fig. 1. Light scattering pattern from a PIPS in a thermoset/thermoplastic blend. The mixture is composed of an epoxy resin (DGEBA), a linking agent (MCDEA) and a thermoplastic (PEI, 5% in weight). The system is cured at 80°C.

from the scattering of the phase separating units, called the form factor, denoted P, and the other resulting from the spatial correlation of the units called the structure factor and denoted S. In most practical cases, P and S can be explicitly calculated and the scattering intensity can be deduced. If, knowing the nature of the scattering units and their spatial positions, it is possible to predict the small angle scattering pattern, then the contrary is not possible ab initio. This opens the way to an important matter of debate, whether it is possible to predict the type of phase separation (SD or NG) from the scattering pattern. It is clear that knowing which mechanism is active in a phase separation is of fundamental importance in order to understand the thermodynamics of the process and also in order to tailor the final morphology of materials.

One area where such an approach is important is the polymerisation induced phase separation (PIPS). It is a technique commonly used for preparing polymer composites [16–18]. At the beginning of the process, the mixture is homogeneous. The increase of the average molar mass of a polymerising component will induce the phase separation mainly by changing the mixing entropy. The final structure is controlled by the competition between the phase separation and the increase of the viscosity of the matrix. At a certain point, the matrix vitrifies and the structure is nearly frozen.

Light scattering has been widely used to study PIPS [19–27] with two opposing interpretations of the light scattering patterns. In most cases, the light scattering patterns are in the form of a scattering ring, which changes its intensity and angular position as the phase separation advances. Fig. 1 gives a typical example of such a ring pattern, taken during the curing of a thermoset/thermoplastic mixture. Depending on the system and experimental conditions, the ring is more or less pronounced and its angular position depends on the spatial extent of the phase separation. All controversy is in the scattering arrangement that can produce such a ring. Several papers ascribe such a ring unambiguously to an SD process [4,23–26]. It is known and well understood that an SD process will give a ring. The way in which this ring changes its intensity and angular position proceeds in three phases [27]. In the early stage, periodic concentration fluctuations with wavelength Λ are built up throughout the whole sample. The amplitude of the fluctuations increases with time while Λ is nearly constant. A scattered ring appears. In the intermediate stage, the concentration fluctuations grow. Hence, the amplitude and the wavelength of the fluctuations grow. The ring brightens and collapses. When the equilibrium concentrations in each phase are reached, the system enters the final stage. In this period, the domains grow in size in a self-similar way and their boundaries are sharpened.

Recently, a group showed that a ring similar to that observed in PIPS can also be explained by an NG process [28]. Their analysis is based on two different approaches. The first approach considers the growth of spatially distant spheres (i.e. the structure factor is ignored) that are surrounded by a depleted zone. In agreement with previous similar results [29,30], this analysis shows that a ring can be produced. The way in which the intensity and position of the ring change depends on the complex coupling between the phase separation rate, the polymerisation rate and the change in diffusion coefficient of the A and B species as a function of A and B concentrations. The second approach [31] considers the case of growing spheres that will come closer and closer. In that case, both the form factor and the structure factor have to be taken into account. Using a detailed analysis of the PIPS thermodynamics, the authors show that a quench into the metastable region may produce an NG phase separation that will give a scattering ring similar to the one classically observed in PIPS and previously ascribed to an SD mechanism. Their analysis is based on the coupling of a form factor and a structure factor since the spheres will be close to each other. This very classical approach uses the most simple structure factor (that will be also used in this paper and described in detail later) that produces a coherence peak at a given scattering angle in all directions, thus giving rise to a ring. The peak coming from the structure factor increases as the spatial coherence increases, as it occurs when the phase separation advances. A careful look at this paper shows that the authors consider a very special case. The size (or the mean size when considering the polydispersity) is changing by a very minor amount between the beginning of the phase separation and a conversion (or a time) where the size is fixed, while the concentration of spheres continues to increase. This has two consequences. The first concerns the light scattering pattern that is nearly completely controlled by the structure factor known to produce a ring. The second is that in the monodisperse case (spheres with all the same size),

fixing the size and increasing the concentration imply an instantaneous, impossible, growth of spheres of a fixed size.

Recognising the importance of being able to know by SALS which mechanism (SD or NG) causes a phase separation, it is necessary to investigate this matter more thoroughly. The aim of this paper is to show that NG and SD cannot be confused, even if in some cases, both can lead to a light scattering pattern in the form of a ring. To do this, the SALS corresponding to the growth of isotropic spheres during a phase separation process, will be modelled using a complete light scattering theory (Mie) and taking into account spatial coherence and multiple scattering. When a ring appears, its behaviour as a function of time will be analysed and compared to that known to occur for an SD process, in order to see if both can be confused.

2. Phase separation model

Phase separation can take two different morphological and thermodynamical routes, NG and SD. Since the light scattering by SD is known to give a scattering halo that is well documented, we will focus in this paper on the NG process, which can give several different types of SALS patterns, depending on the size and concentration of the growing nuclei.

The NG mechanism is one of the processes throughout which a polymer blend, initially homogeneous, may enter phase separation. This mechanism takes place in the metastable region of the phase diagram of the system. Small nuclei are formed by random variations in concentration. A nucleus will grow only if its radius is larger than the critical radius. Nuclei smaller than the critical size will disappear because the decrease in free energy does not compensate for the excess in surface energy. In general, the composition of the nucleus is fixed by thermodynamics and is constant during the growth process. For the PIPS, the composition of the nucleus is varying with time since the conversion is increasing. The resulting morphology is a two-phase system with a droplet structure. This means that polydisperse spheres are randomly dispersed in the matrix. In NG, the average size of the nuclei and droplets are determined by kinetics, but the amplitude of the fluctuations, i.e. the concentration difference between the two phases is determined by the thermodynamic conditions of the mixture. In general, during the NG process, nuclei are born at random time (heterogeneous NG) or simultaneously (homogeneous NG) and grow from then on. In our calculations, the NG process is either homogeneous (the spheres are created at the same time and they grow in the same way) or heterogeneous (the spheres are created at various time, and the resulting morphology is a distribution of spheres with various sizes).

The growth can be described as the evolution of size as a function of time. Most models and experiments follows a law as [32–34]:

$$R(t) = R_0 t^m \tag{3}$$

where R is a size of the sphere (radius), R_0 the initial size and m an exponent usually in the range of 0.3–0.6. The value of the exponent changes the evolution of the scattering pattern with absolute time. As seen later, this may be important when comparing the SD and the NG processes.

During the phase separation, the two phases change their composition. To simplify calculation, since this paper does not refer to a given phase diagram, we will keep the refractive index of the growing sphere constant since its composition does not change much. This approximation changes slightly the variation of the intensity of the scattering light. Doing this, we have to vary the refractive index of the medium.

Consider a mixture of components A and B with concentrations ϕ and $(1-\phi)$, respectively, and refractive indexes n_A and n_B. The refractive index in the mixture is taken as $n_{mix} = n_A\phi + n_B(1-\phi)$. ϕ can be calculated using the initial concentration of A in the mixture ϕ_A (without any phase separation having taken place), the concentration of A in the sphere ϕ_α, the total volume of spheres V_α and the total sample volume V_{tot} as:

$$\phi = \frac{\phi_A V_{tot} - \phi_\alpha V_\alpha}{V_{tot} - V_\alpha} \tag{4}$$

Having set these parameters, we have a general model that is valid for the phase separation of systems with no additional chemical reaction and a good approximation of the case of PIPS. Implementation of the parameters size evolution as a function of time, volume fraction of the spheres and composition of the two phases of a real PIPS poses only, in practice, the problem of measurement and calculation.

3. Light scattering approach

As has been mentioned, the scattered intensity, I_s is the result of the contribution of the form (P) and of the structure (S) factors:

$I_s \propto PSI_0$, with I_0, the incident intensity. In what follows, the form and the structure factor will be expressed explicitly.

3.1. Mie scattering of an isolated sphere

Using electromagnetic theory (Maxwell's equations and proper boundary conditions) Gustav Mie obtained in 1908 an exact solution for the scattering of a plane monochromatic wave by an isotropic sphere embedded in an isotropic medium [35]. Although this formal solution has been around for many years, it has been a practical means for detailed computations only since the advent of computers.

In order to calculate the intensity scattered by a homogeneous sphere in a homogeneous medium, Mie proposes to link the components of an incident electromagnetic plane

wave with its scattered ones via a transfer matrix. Only the resulting formulas of Mie theory for the calculus of the coefficients of this matrix are given here. For a detailed derivation, the reader is referred to literature [36–38].

The amplitude functions can be expressed as:

$$S_1(\theta) = \sum_{n=1}^{\infty} \frac{(2n+1)}{n(n+1)}[a_n\pi_n(\cos\theta) + b_n\tau_n(\cos\theta)]$$

$$S_2(\theta) = \sum_{n=1}^{\infty} \frac{(2n+1)}{n(n+1)}[b_n\pi_n(\cos\theta) + a_n\tau_n(\cos\theta)] \quad (5)$$

$$S_3(\theta) = S_4(\theta) = 0$$

The functions $\pi_n(\cos\theta)$ and $\tau_n(\cos\theta)$ can be calculated as:

$$\pi_n(\cos\theta) = \frac{dP_n(\cos\theta)}{d\cos\theta}$$

$$\tau_n(\cos\theta) = \cos\theta\,\pi_n(\cos\theta) - \sin^2\theta\frac{d\pi_n(\cos\theta)}{d\cos\theta} \quad (6)$$

in which $P_n(\cos\theta)$ is the Legendre polynomial.

The Mie coefficient a_n and b_n equal:

$$a_n = \frac{\Psi'(mx)\Psi_n(x) - m\Psi_n(mx)\Psi'_n(x)}{\Psi'_n(mx)\zeta_n(x) - m\Psi_n(mx)\zeta'(x)}$$

$$b_n = \frac{m\Psi'_n(mx)\Psi_n(x) - \Psi_n(mx)\Psi'_n(x)}{m\Psi'_n(mx)\zeta_n(x) - \Psi_n(mx)\zeta'_n(x)} \quad (7)$$

In this formula:$x = (2\pi a)/\lambda$ is the dimensionless size parameter (a the radius of the sphere, λ the wavelength of the light in the medium). $m = n_1/n_2$ where n_1 is the refractive index of the sphere and n_2 the refractive index of the medium.

The Riccati–Bessel functions $\Psi_n(z)$ and $\zeta_n(z)$ are defined as:

$$\Psi_n(z) = \sqrt{\frac{\pi z}{2}}J_{n+1/2}(z);$$

$J(z)$ is the Bessel function from the first kind.

$$\zeta_n(z) = \sqrt{\frac{\pi z}{2}}H^{(2)}_{n+1/2}(z);$$

$H^{(2)}(z)$ is the Bessel function from the second kind. (8)

The scattered intensity becomes I_{VV} or I_{HV} whether the sphere is placed between polariser and analyser parallel or crossed. In the small wave vector [37], the resulting intensities are:

$$I_{VV} = \frac{|S_1\sin^2\mu + S_2\cos^2\mu|^2}{k^2r_0^2} * I_0 = P_{VV\text{–}Mie} * I_0$$

$$I_{HV} = \frac{|S_1 - S_2|^2\sin^2(2\mu)}{4k^2r_0^2} * I_0 = P_{HV\text{–}Mie} * I_0 \quad (9)$$

where μ is the azimuthal angle on the diffusion pattern, and I_0 the incident intensity. In what follows, only the VV situation will be considered since the depolarised part is negligible for an isotropic situation.

3.2. Multiple scattering

In a real situation, multiple scattering is a correction that has to be made to Mie theory. Actually, one never works with one sphere but with a cloud of spheres. Each particle in the sample is not only exposed to the light from the incident beam but also to the light scattered by the other particles. Before arriving at a particle, the original beam may also have suffered extinction by other particles. If these effects are strong, multiple scattering cannot be neglected. In general, multiple scattering causes a broadening and flattening of the scattering profile.

Theories for multiple scattered light belong to two classes. The first class involves a radiative transfer approach. The second class is based on the determination of the successive angular intensity distributions of each order of scattering. We will treat only the second class here. A general theory due to Hartel [39] and extended by Woodward [40] is presented. The general idea of this method is to take into account that light scattered by one particle can meet other particles before leaving the sample. Hartel's idea is to consider that the moment the light scattered by one particle meets another particle, it is scattered again according to the single scattering distribution. In this way, double scattering represents the single scattering of the "single scattered" light. In order to formulate this theory, a specific formalism is used. The theory presented here is only valid at an azimuthal angle of 45°. In literature, a theory has been proposed to take into account the azimuthal dependence, too, and to build a multiple scattering version of any other scattering theory, that of Mie or an approximation [41].

In practice, the sample is divided into successive imaginary parallel layers of the same thickness, delta z. As the incident intensity travels along a layer, a portion of its energy, $Q_k(z)$, is distributed over the scattering angle θ according to the single scattering distribution of Mie, $f_k(\theta)$; k is the order of scattering. As has been mentioned before, it is not our purpose here to detail the complicated expressions of the light quantities and of the angular distribution functions. All these equations can be found in literature [39–42].

The total angular distribution for the scattered light at z is obtained by summation over all light scattering orders and is:

$$I_{tot} = \sum_{k=1}^{\infty} Q_k(z)f_k(\theta) \text{ with } Q_k(z) = \frac{(\tau z)^k}{k!}e^{-\tau z},$$

τ being the turbidity of the sample and

$$f_k(\theta) = \frac{1}{4\pi}\left[1 + \sum_{n=1}^{\infty}\frac{c_n^k}{(2n+1)^{k-1}}P_n(\cos\theta)\right] \quad (10)$$

$P_n(\cos\theta)$ are Legendre polynomials. Another formulation of Mie theory is used here. Chu and Churchill [42] derived expressions to calculate the coefficients c_n (related with the a_n and b_n coefficients of the Mie theory).

3.3. Non-independent scattering of spheres

Up till now, we have considered that waves scattered by different particles from the same incident beam in the same direction may not interfere. Independent scattering means that there is no systematic relation between the phases of these waves. This condition is only met in dilute systems, in which there is a random distribution of the scatterers. In more concentrated systems, intensities cannot simply be added. Intensity must take into account $S(q)$, the structure factor, which accounts for the interparticle interference. $S(q)$ will be equal to 1 at all q for low concentrations.

For monodisperse particles, $S(q)$ is given by [43,44]:

$$S(q) = 1 + 4\pi N \int_0^\infty (g(r) - 1)\frac{\sin(qr)}{qr} r^2 \, \mathrm{d}r \tag{11}$$

where $q = ((4\pi)/\lambda)\sin(\theta/2)$ is the wave vector, λ the wavelength of the electromagnetic wave in the medium, N the particle number density and $g(r)$ the radial distribution function describing the arrangement of the particles.

In liquid, one mostly uses the total correlation function, defined as:

$$h(r_{12}) = g(r_{12}) - 1 \tag{12}$$

which measures the deviation of the pair distribution function from its background value due to the influence of particle 1 on particle 2 at a distance r_{12}. A successful approach is to consider $h(r_{12})$ as consisting of a direct correlation between particles 1 and 2 and an indirect term by which the correlation is transferred to all neighbouring particles. This is expressed mathematically as:

$$h(r_{12}) = c(r_{12}) + N \int c(r_{13})h(r_{32}) \, \mathrm{d}r_3 \tag{13}$$

An often-used approximation for the direct correlation function is the Percus–Yevick [45] expression, valid for monodisperse hard spheres in a liquid:

$$c(r) = (\mathrm{e}^{-\phi(r)/\mathrm{kT}} - 1)\,\mathrm{e}^{\phi(r)/\mathrm{kT}} g(r) \tag{14}$$

$$\text{with } \phi(r) = \infty \text{ for } 0 < r < 2R \text{ and } \phi(r) = 0 \text{ for } r > 2R$$

R is the radius of the spheres. Because $c(r)$ is a correlation between particles 1 and 2, it falls off quickly to zero with separation distance.

Solving these equations finally results in [43,46]:

$$S(q) = \frac{1}{1 + 24\eta G(A)/A} \tag{15}$$

where $A = 2qR$, $\eta = (4\pi R^3 N)/3$ is the hard sphere volume fraction, and

$$G(A) = \frac{\alpha}{A^2}(\sin A - A\cos A) + \frac{\beta}{A^3}(2A\sin A + (2 - A^2)\cos A - 2) + \frac{\gamma}{A^5}(-2A^4\cos A + 4[(3A^2 - 6)\cos A + (A^3 - 6A)\sin A + 6)] \tag{16}$$

where

$$\alpha = \frac{(1 + 2\eta)^2}{(1 - \eta)^4}$$

$$\beta = \frac{-6\eta(1 + \eta/2)^2}{(1 - \eta)^4}$$

$$\gamma = \frac{1/2\eta(1 + 2\eta)^2}{(1 - \eta)^4}$$

3.4. Scattering during a spinodal decomposition

The scattering during an SD process is well known. The early stages of SD can be described by the Cahn–Hilliard linearised theory [2,47]. Starting from a diffusion equation, this theory gives an expression of the structure factor. The evolution of the structure factor with time is characterised by an exponential growth with a fixed maximum located around q_m, the wavevector referring to the dominant mode of fluctuation concentration.

Langer, Bar-on and Miller gave a more general expression of the evolution of the structure factor, taking into account the non-linearities contained in the diffusion equation [48]. The model predicts, in the intermediate stages of the SD, an evolution of the scattered peak to the small wavevectors. This evolution corresponds to the growth of the domains. As the concentration fluctuations grow, the amplitude of the fluctuations grows. At the moment the equilibrium concentrations in each phase are reached, the system enters the final stage.

In the final stage of SD, the self-similar growth of the morphology [5] is observed. It is thus useful to define a scaled structure factor $F(x,t)$ in the following way [49]:

$$F(x,t) = I(q,t)q_m^d(t) \tag{17}$$

where $x = q/q_m(t)$ and $d = 3$ for a 3D system. In the final stages of the SD, $F(x,t)$ is assumed to be independent of time. Binder and Stauffer propose also scaling rules to describe the scattered intensity [49,50]:

$$q_m(t) \propto t^{-\alpha} \qquad I_m(t) \propto t^{\beta} \tag{18}$$

where I_m is the scattered intensity at q_m. The theory predicts the $\beta = 3\alpha$ relation between the scaling exponents. However, sometimes, these power laws concerning the evolution of the maximum intensity $I_{\max}$ and its associated

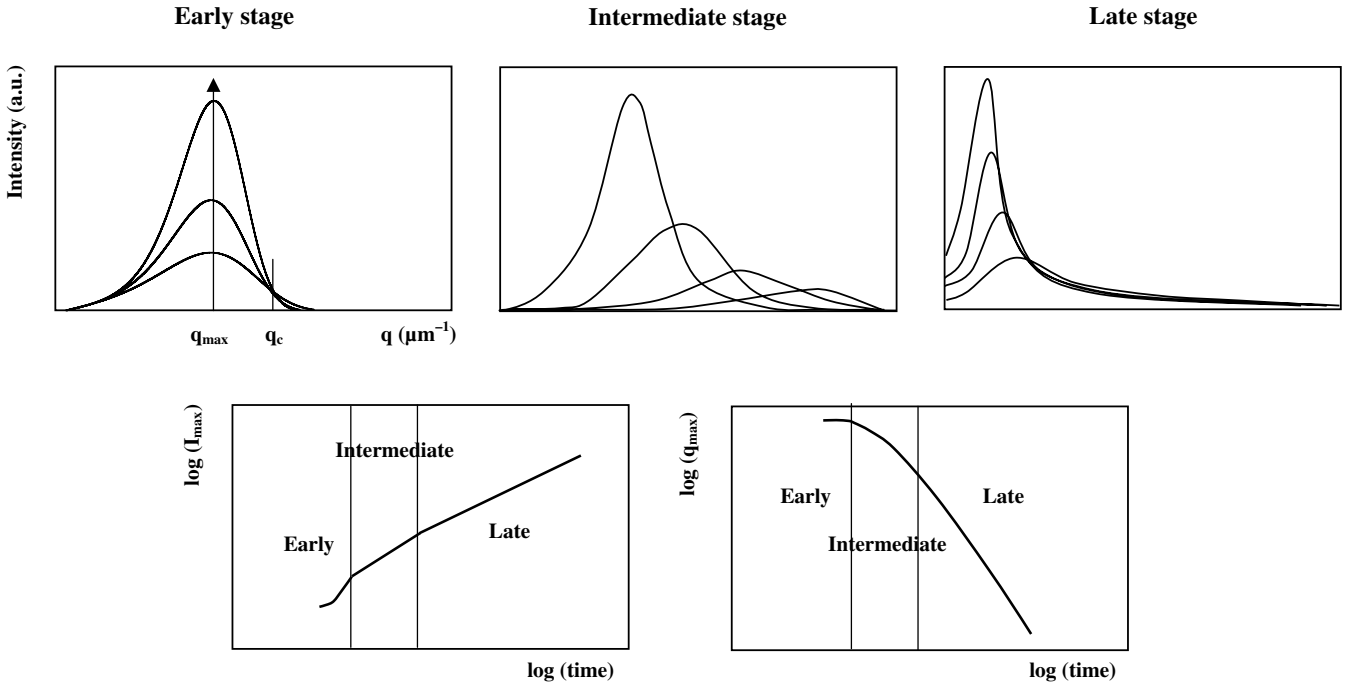

Fig. 2. Schematic drawing of the evolution of the scattering peak during spinodal decomposition.

wave vector q_m during the final stages of SD are not considered. In fact these scaling laws work in the case when the phase separation does not imply any chemical reaction, like the polymerisation of one of the components of the blend where the increase in the viscosity of the blend can restrict the evolution of the morphology. The evolution of the structure factor during SD is summarised in Fig. 2.

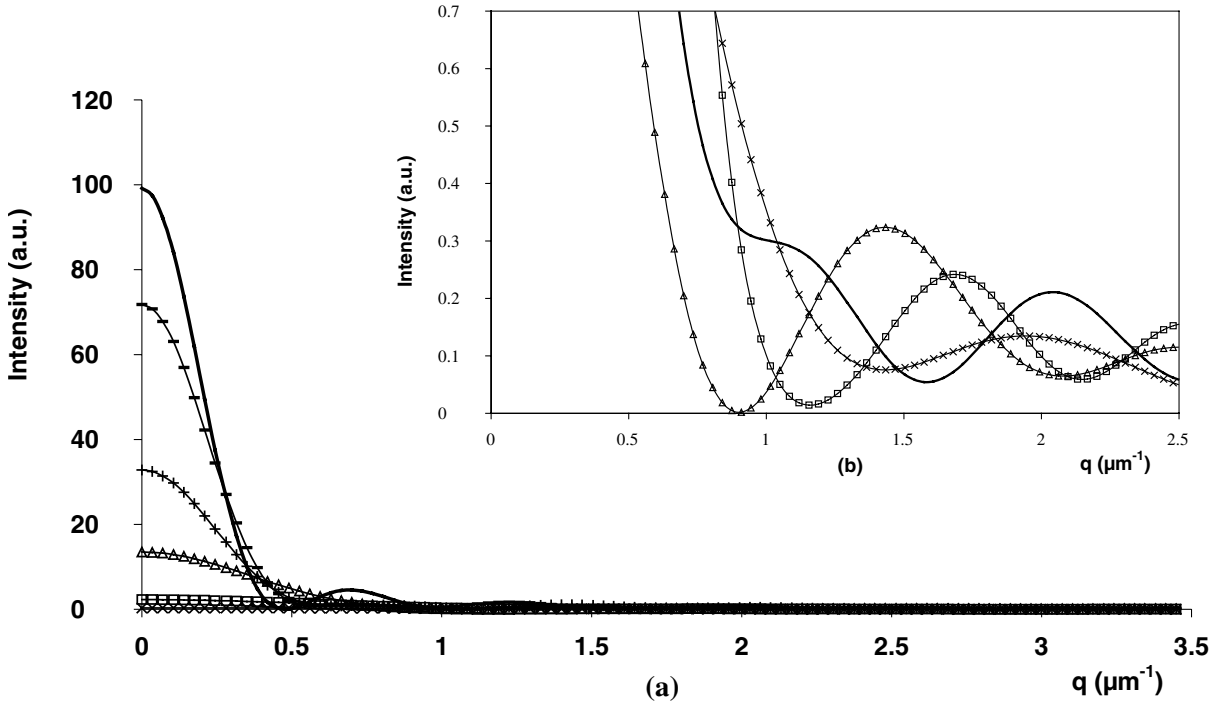

Fig. 3. (a) NG simulation. Initial radius of the sphere 1 μm, exponent in growth law 0.5, refractive index of components A and B 1.55 and 1.33, respectively, concentration of A in the sphere 0.95 and 0.3 in the homogeneous mixture. With time, the radius of the spheres is increasing. Radius of the spheres, in micrometres: (– × –) 1.00; (–□–) 1.73; (–△–) 3.00; (– | –) 4.12; (–■–) 5.00; (—) 5.74. (b) Details of (a). Disappearance of the second-order peak. Radius of the spheres, in micrometres: (– × –) 1.73; (–△–) 2.24; (—) 2.65; (–□–) 3.00.

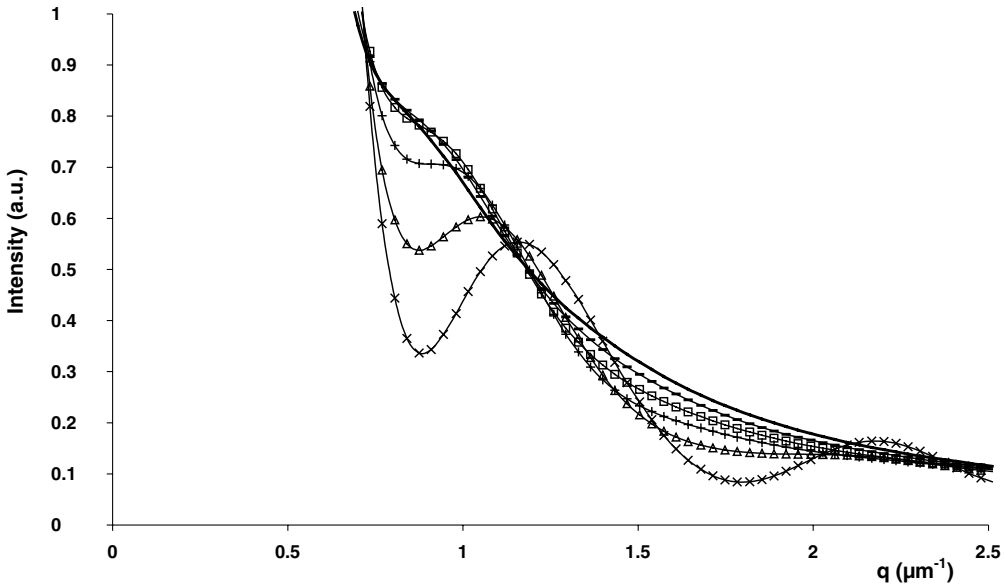

Fig. 4. Effect of polydispersity. Mean radius of the sphere 3.3 μm. The relative polydispersity is indicated: (– × –) 4%; (–△–) 8%; (– | –) 12%; (–□–), 16%; (–■–) 20%; (—), 24%.

4. Results and discussion

4.1. Computation parameters

In the following, we present simulations of light scattering profiles that should be encountered during NG. Different situations will be considered, starting from the case of an isolated sphere and an assembly of polydisperse spheres. Then more realistic experiments will be examined taking into account the influence of multiple scattering and of the structure factor for a dense population of spheres. The purpose is to show how the scattering patterns evolve as the phase separation proceeds, under which conditions they can exhibit a non-zero-angle peak and how this peak behaves. The choice of the simulation parameters is described below. For the sake of comparison of all the different conditions, the nuclei will have an initial radius of 1 μm in all simulations. The choice of the growth rate is important because it influences the time evolution of the scattering patterns and thus the evolution in the positions of the peaks. As for most real situations, the exponent of the growth law is taken to be equal to 0.5 [32].

4.2. Growth of an isolated sphere (Mie theory only)

Fig. 3a and b shows the scattering intensity due to the growth of a single sphere during a phase separation process. The refractive indexes of components A and B are 1.55 and 1.33, respectively. The refractive index of the sphere is 1.55 and the concentration of A in the mixture was 0.3 before phase separation. The refractive index of the medium is 1.39 at the beginning of the simulation and decreases with time.

The figures show the typical behaviour that we expect from Mie curves: a maximum intensity in the centre of the pattern, decreasing as the angle increases but with some secondary maxima. Let us see if this secondary maximum could be confused with what occurs during an SD. The evolution of the position and intensity of the second maximum is not monotonic. In general, the second maximum goes to smaller angles with increasing time. However, sometimes, the second maximum jumps instantaneously to a larger angle. In fact, as the second maximum evolves towards the centre of the image, it will come closer and closer to the powerful first maximum intensity peak at zero-angle. At a certain moment the second maximum will disappear in this central peak. It appears as if the second maximum is swallowed by the first peak (Fig. 3b for a sphere with a radius of 2.65 μm). The new apparent second maximum is then displaced to wider angles. The third maximum in $P(q)$ becomes the second one, and so on. This phenomenon has to be taken into account during an analysis of a scattering pattern in order not to make mistakes in the positions of the peaks. Anyway, even if the zero-angle peak is not taken into account, the "apparently" random evolution of the position of the second maximum cannot be mistaken with the continuous evolution of the peak generated by an SD to the small wavevectors.

4.3. Growth of polydisperse spheres

In general, if no special care is taken to disperse in the material a nucleation agent (this is very common for crystallisation, but not really for PIPS), the nucleation will be heterogeneous with a polydispersed resulting morphology. The influence of the polydispersity on the scattering patterns was also studied. The particles are not supposed to have the same size. The program supposes the radius distribution to be gaussian. An average intensity profile is

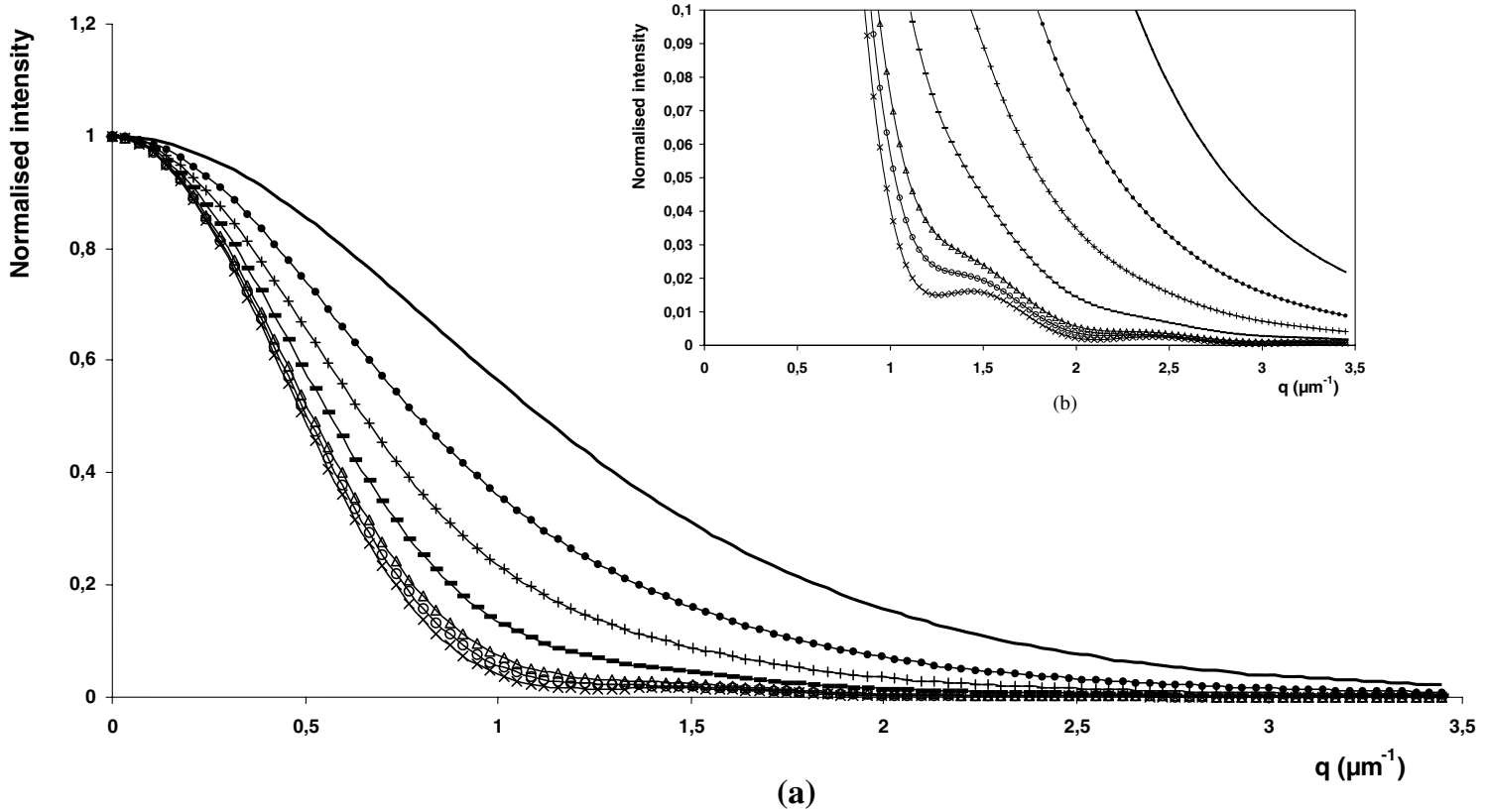

Fig. 5. (a) Effect of multiple scattering, normalised intensity. Parameters: diameter of spheres 5 μm, refractive index 1.5 for the sphere and 1.45 for the medium, 10% (vol.) of spheres and different thickness of the sample as indicated: (– × –) 5; (–○–) 10; (–△–) 15; (–■–) 30; (– | –) 50; (–·–) 75; (—) 150. (b) Details of (a). (c) Effect of multiple scattering, non-normalised intensity. Same parameters as in (a). Thickness of the sample as indicated: (– × –) 5 μm; (–◇–) 10 μm; (–△–) 15 μm; (–■–) 30 μm; (– | –) 50 μm; (–●–) 75 μm; (—) 150 μm.

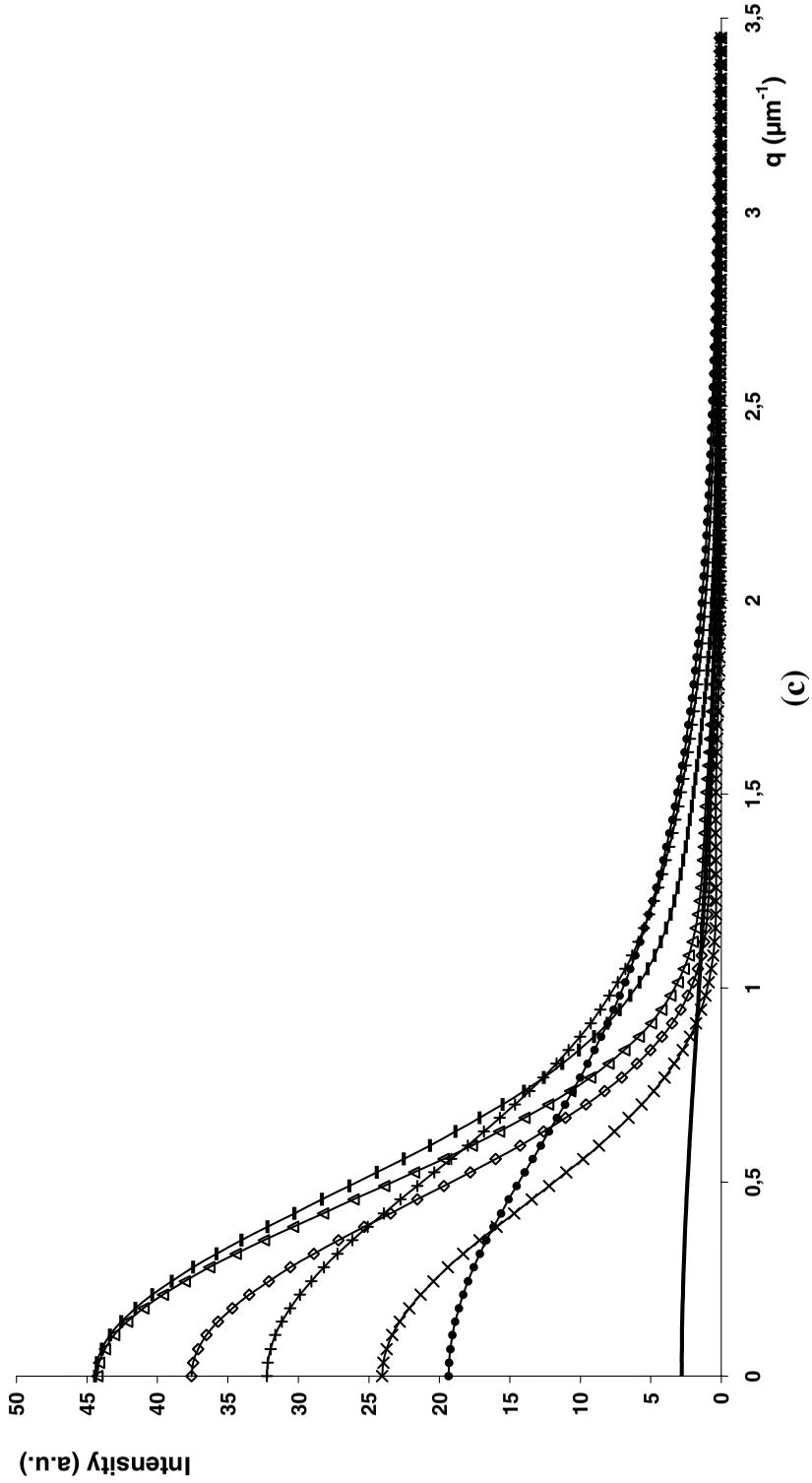

Fig. 5. (*continued*)

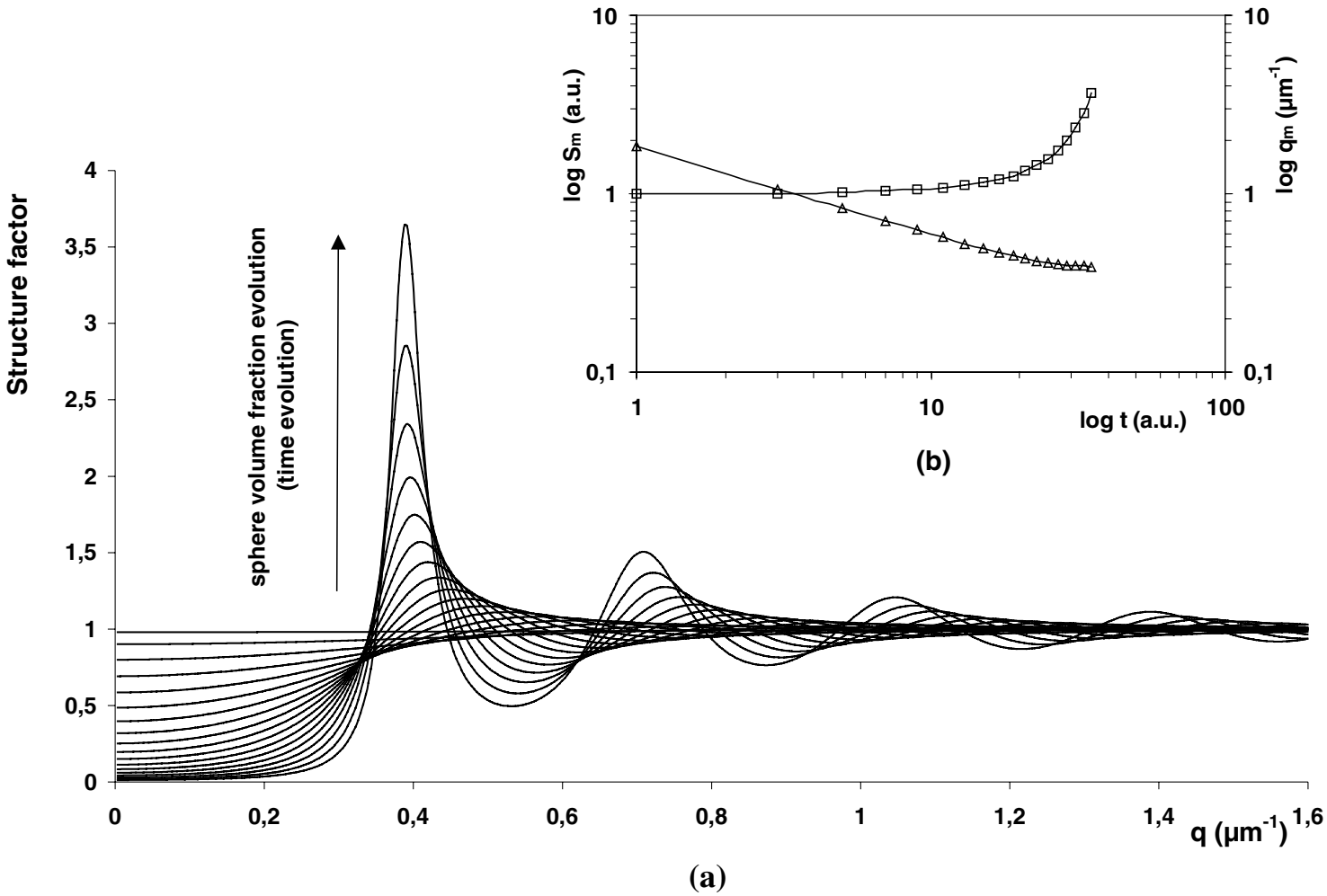

Fig. 6. (a) Evolution of the Percus–Yevick structure factor during the NG process. From 0 to 52% of sphere volume fraction. (b) Evolution of the intensity and of the wavevector of the first maximum of the structure factor: (–□–) Im; (–△–), qm.

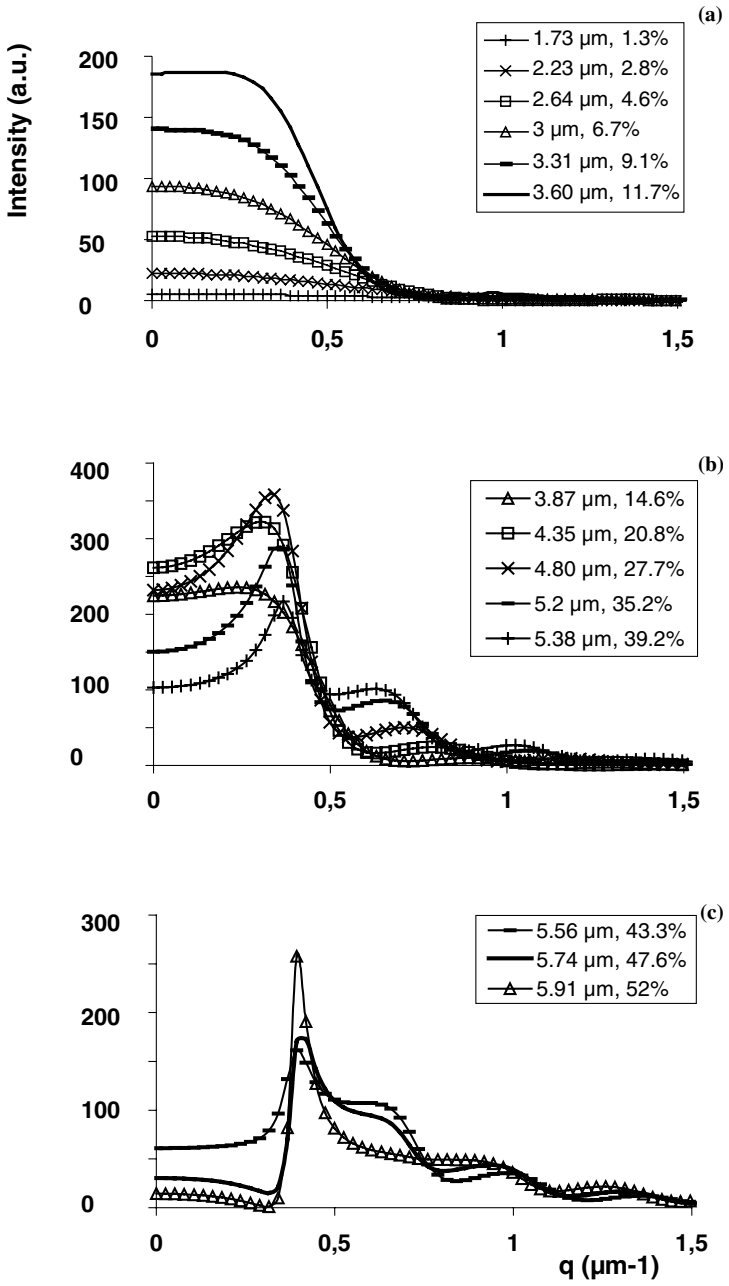

Fig. 7. NG simulation. Influence on the Mie profile of the Percus–Yevick structure factor. Different sphere volume fractions as indicated.

then extracted from each Mie curve corresponding to the different couples (number of spheres, radius) on the gaussian distribution.

No particular behaviour of the second-order maximum is observed. Here again, the scattering patterns are very different from those observed in the case of an SD. Fig. 4 compares results for different levels of polydispersity when the mean radius of the spheres of the previous simulation reaches 3.3 μm. As expected, increasing polydispersity causes the second maximum to be less pronounced and finally to disappear. The second maximum is observable up to 16% polydispersity. Up to 8% the third maximum is observable, but higher-order maxima disappear very quickly and cannot be distinguished for a polydispersity greater than 4%. So, even a relatively small polydispersity smears out secondary scattering peaks, rendering a potential confusion with SD impossible.

4.4. Growth of spheres with multiple scattering

Multiple scattering is sometimes inevitable, especially when the size of the growing spheres is much smaller than the size of the container. Fig. 5a shows the effect of multiple scattering for spheres with radius 2.5 μm, refractive index 1.50 for the sphere and 1.45 for the medium. The sample contains 10% (vol.) of spheres and we vary the thickness of

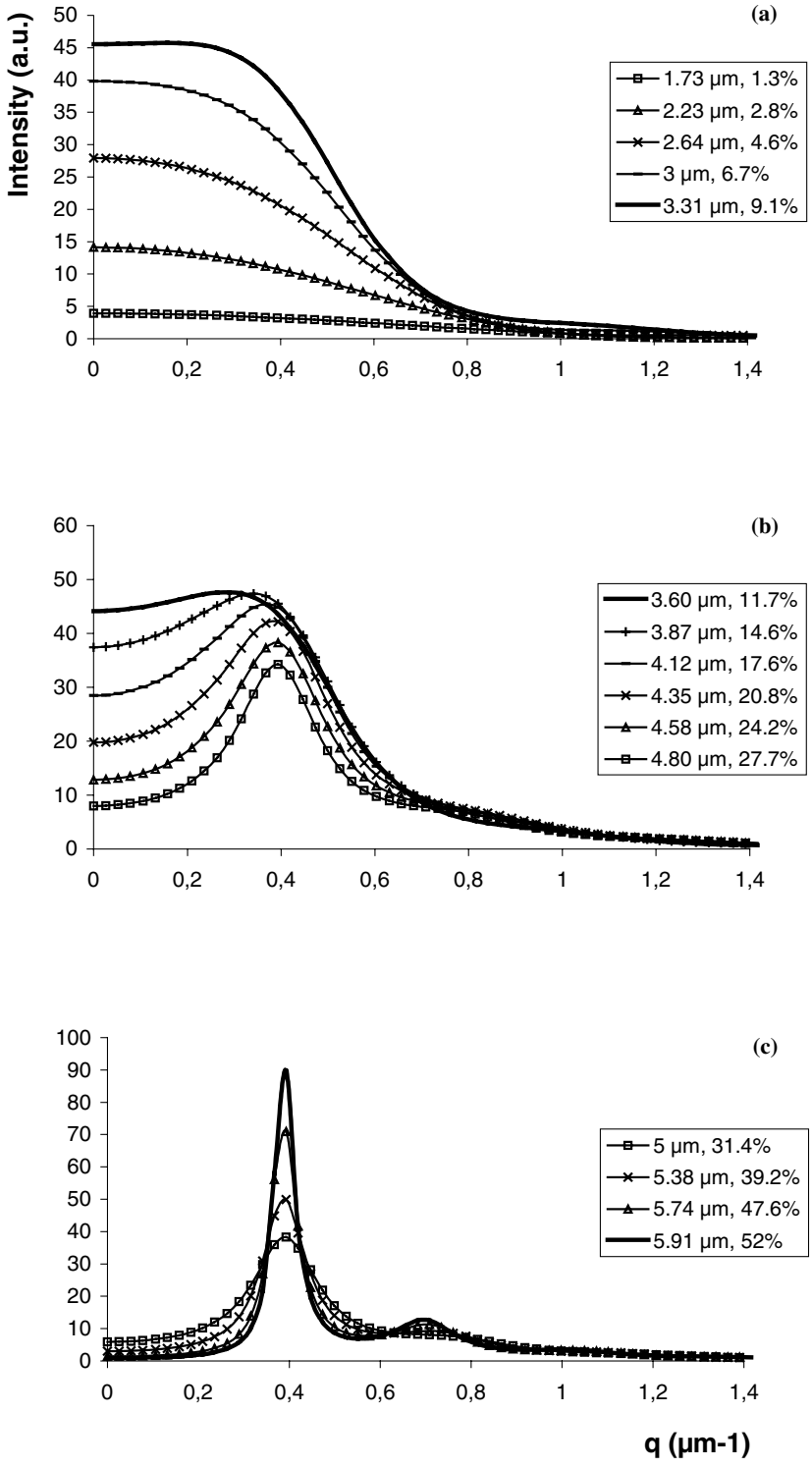

Fig. 8. Mie theory + multiple scattering + structure factor. Thickness of the sample 30 µm. Different sphere volume fractions as indicated.

the sample to account for multiple scattering. The curves are normalised. If the sample thickness increases, multiple scattering becomes more important. At first, the main effect is the disappearance of all the second-order peaks predicted by Mie theory (details in Fig. 5b). If the thickness increases further, the flattening effect continues. Besides this effect, there is a second consequence of multiple scattering, which concerns the global intensity. Fig. 5c contains the same profiles as the previous figure but the intensities are no longer normalised. In increasing the sample thickness in an SALS experiment, at first scattered intensity will increase because there are more scatterers (thickness from 5 to

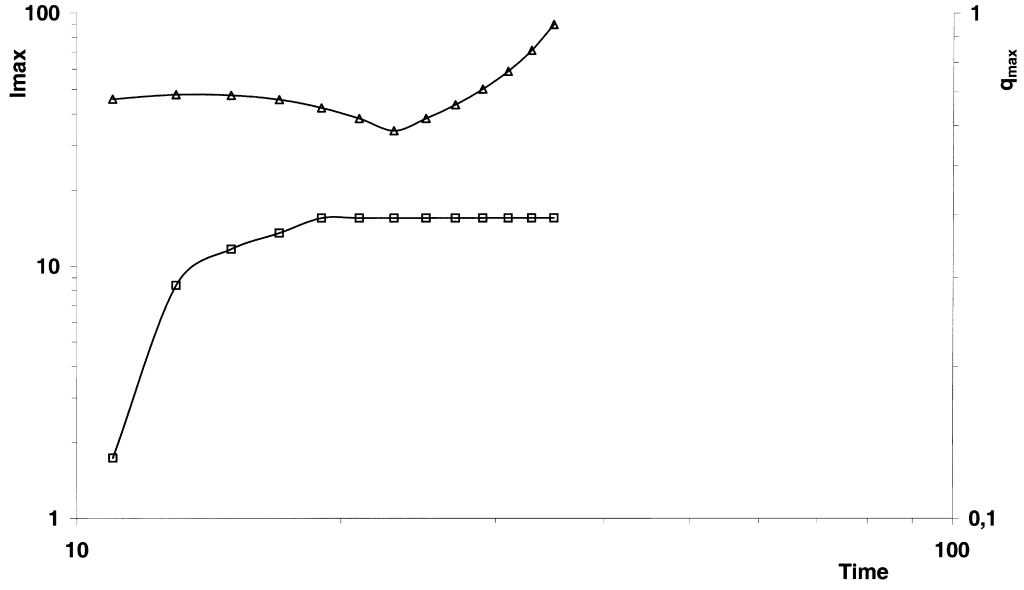

Fig. 9. Evolution of the maximum of intensity and of its associated wavevector, for the case of Fig. 8. (–△–) I_m; (–□–) q_m.

30 μm in this example). If the thickness increases further, the observed intensity at small angles will decline because a large part of the intensity is scattered at large angles due to multiple scattering (thickness >30 μm in the example). From these results it is now possible to know how thin the sample should be or how low the concentration should be in the sample to avoid large multiple scattering effects. The general effect of multiple scattering is to depress secondary maxima and is adverse to a potential confusion with SD.

4.5. Simulations based on non-independent scattering

We have shown so far that the scattering of monodispersed, polydispersed, with or without multiple scattering cannot produce a ring with no intensity at zero scattering angle, but can produce secondary maxima that are more pronounced for monodispersed spheres with no multiple scattering. Nevertheless, we have shown that the evolution of these secondary maxima is not monotonic with time as the phase separation progresses because of the complex influence of the changes of sizes and relative refractive indexes on the Mie theory. There is thus no possibility to confuse these peaks with what is happening in an SD. We will turn now to a more potential actor in a possible confusion between NG and SD, i.e. when the spheres start to be so close that independent scattering is no longer valid. In that case, we have to add to the individual scattering a structure factor such as the one given in the theory part and illustrated in Fig. 6a. For this simulation, the refractive index of the A and B components are 1.6 and 1.5, respectively, and the concentration of component A is taken to be equal to 0.7 before phase separation. Fig. 6a shows the well-known result of a series of peaks positioned at finite scattering angles. With the increase of the phase separation in time (evolution of the refractive indexes, of the size of the spheres and of sphere volume fraction), the peaks grow in intensity and move in position (see Fig. 6b for the details). Let us now couple this structure factor to the Mie form factor of the spheres, as given before, by multiplying the two terms (a procedure valid only for spherical particles). An example of this is given in Fig. 7. At low conversion, the scattering is not affected by the interparticle interactions. For this example, there is no influence of interparticle interactions below a concentration of 10%. Above 10%, the effect of the interparticle interactions is mainly to decrease the scattering at low angles and to smear it out at large angles. The created peak seems to have no particular evolution, either in intensity or in position, and thus cannot be mistaken with the peak occurring during an SD. This behaviour is mainly due to the evolution of the width of the central peak superimposed with the maximum of the structure factor. The higher-order peaks are a combination of the orders peaks of the structure factor and of the orders moving peaks due to the single scattering of the spheres. Moreover, it can be shown that the appearance and the evolution of this peak strongly depends on the material parameters (refractive indexes, initial composition of the blend).

4.6. Growth simulation including non-independent and multiple scattering

We present here a complete simulation of growth of spheres (see Fig. 8). It takes into account the influence of multiple scattering and of the structure factor. In order to demonstrate the effect of the above corrections on a realistic case, the refractive indexes of A and B components are taken to be equal to 1.6 and 1.5, respectively. These values correspond to some current ones for polymer blends. The initial mixture contains 70% of component A and 30% of component B. The initial refractive index of the medium is

1.57. The thickness of the sample is taken to be equal to 30 μm.

At first, the traditional zero-angle peak predicted by the Mie theory increases till the time the spheres reach a radius of 3.31 μm. This time corresponds to a sphere volume fraction of 9.1%. In a second time, owing to the influence of multiple scattering, this intensity decreases and a peak appears at a non-zero angle. Then, the influence of the structure factor leads to a narrow peak (sphere volume fraction of 27.7% and sphere radius of 4.8 μm). Let us now look at the evolution of the maximum of intensity and its associated wavevector from its appearance (see Fig. 7b). The curves of Fig. 9 doubtless cannot be assigned to an SD process where the wavevector corresponding to the maximum of intensity continuously evolves to the small values.

5. Conclusions

Theoretical predictions of light scattering patterns associated with the nucleation and growth (NG) phase separation mechanism were presented. Non-independent and multiple scattering, which can play a role in practical situations, were taken into account. A continuous evolution in the position of the scattering peaks has been shown. Moreover, as in the case of a spinodal decomposition (SD), it is possible to obtain a peak at a non-zero angle. However, an important statement has to be made. In the spinodal case, this peak first appears at a finite angle before evolving to the small angles, whereas in the NG case, a zero-angle peak is already present at the beginning of the process. Then, the intensity of this peak decreases, and a peak, mainly resulting from the structure factor of the spheres, appears. This comparison of the evolution of the scattering patterns constitutes the way to discriminate between the two phase-separation processes. There should not be any possible confusion between SD and NG processes, and small angle light scattering should be able to tell which process is active.

Acknowledgements

Tom Van Nuland thanks the Erasmus program of the European Community for support.

References

[1] Komura S, Furukawa H, editors. Dynamics of ordering processes in condensed matter. New York: Plenum Press, 1983.
[2] Gunton JD, San Miguel M, Sahni PS. In: Domb C, Lebowitz JL, editors. Phase transition and critical phenomena, vol. 8. New York: Academic Press, 1983.
[3] Lansac Y. Transition et séparation de phase dans les systèmes cristaux liquides. Thèse de doctorat, Université de Nice (France), 1993.
[4] Hashimoto T. Phase Transitions 1988;12:47.
[5] Inoue T. Prog Polym Sci 1995;20:119.
[6] Langer JS. Ann Phys 1971;65:53.
[7] Langer JS. Ann Phys 1969;54:258.
[8] Becker R, Döring W. Ann Phys 1935;24:719.
[9] Lifishitz IM, Slyozov. J Phys Chem Solids 1961;19:35.
[10] Sondergaard K, Lyngaae-Jorgensen J. Rheo-physics of multiphase polymer systems. Lancaster: Technomic, 1995.
[11] Okamoto M, Inoue T. Polymer 1994;35(2):257.
[12] Kyu T, Mustafa M, Yang JC, Kim JY, Palffy-Muhoray P. In: Noda I, Rubingh DN, editors. Polymer solutions, blends and interfaces. Amsterdam: Elsevier, 1992. p. 245.
[13] Läuger J, Lay R, Gronski. J Chem Phys 1994;101(8):7181.
[14] Lal J, Bansil R. Macromolecules 1991;24:290.
[15] Läuger J, Lay R, Muas S, Gronski W. Macromolecules 1995;28:7010.
[16] Doane JW, Vaz NA, Wu BG, Zumer S. Appl Phys Lett 1986;48(4):269.
[17] Vaz NA, Smith GW, Montgomery GP. Liq Cryst 1987;146:1.
[18] Riew CK, editor. Rubber-toughened plastics Advances in chemistry series, vol. 222. Washington, DC: American Chemical Society, 1989.
[19] Okada M, Fujimoto K, Nose T. Macromolecules 1995;28:1795.
[20] Kim BS, Chiba T, Inoue T. Polymer 1995;36:67.
[21] Girard-Reydet E, Sautereau H, Pascault JP, Keates P, Navard P, Thollet G, Vigier G. Polymer 1998;39(11):2269.
[22] Baeke L, Thioudelet P, Keates P, Navard P. Polymer 1997;38:5283.
[23] Yamanaka K, Inoue T. Polymer 1989;30:662.
[24] Maugey J, Budtova T, Navard P. In: te Nijenhuis K, Mijs W, editors. The Wiley polymer networks review, vol. 1. New York: Wiley, 1998. p. 411.
[25] Kim JY, Cho CH, Palffy-Muhoray P, Mustafa M, Kyu T. Phys Rev Lett 1993;71(14):2232.
[26] Chen W, Kobayashi S, Inoue T, Ohnaga T, Ougizawa T. Polymer 1994;35(18):4015.
[27] Hashimoto T. In Thomas EL, editor. Material science and technology, structures and properties of polymers, vol. 12, 1993. p. 251.
[28] Eliçabe GE, Larrondo HA, Williams RJJ. Macromolecules 1997;30:6550.
[29] Carpineti M, Giglio M, Degiorgio V. Phys Rev E 1995;51(1):590.
[30] Chen D, Pascault JP, Sautereau H, Vigier G. Polym Int 1993;32:369.
[31] Eliçabe GE, Larrondo HA, Williams RJJ. Macromolecules 1998;31:8173.
[32] Cumming A, Wiltzius P, Bates FS. Phys Rev Lett 1990;65:863.
[33] Lansac Y, Fried P, Maissa P. Phase Transitions 1995;54:23.
[34] Nakata M, Kawate K. Phys Rev Lett 1992;68:2176.
[35] Mie G. Ann Phys 1908;25:377.
[36] Van de Hulst HC. Light scattering by small particles. New York: Wiley, 1957.
[37] Meeten GH. Opt Acta 1982;29:759.
[38] Bohren CF, Huffman DR. Absorption and scattering of light by small particles. New York: Wiley, 1983.
[39] Hartel W. Licht 1940;10:141.
[40] Woodward DH. J Opt Soc Am 1964;54:1325.
[41] Prud'homme RE, Bourland L, Natarajan RT, Stein RS. J Polym Sci 1974;12:1955.
[42] Chu C, Churchill SW. J Opt Soc Am 1955;45:958.
[43] Kinning DJ, Thomas EL. Macromolecules 1984;17:1712.
[44] Mischenko MI. J Quant Spectrosc Radiat Transfer 1994;52:95.
[45] Percus JK, Yevick GJ. Phys Rev 1958;110:1.
[46] Pedersen JS. Adv Colloids Interface Sci 1997;70:171.
[47] Cahn JW. Acta Metall 1961;9:795.
[48] Langer JS, Bar-on M, Miller HS. Phys Rev A 1975;11:1417.
[49] Binder K. Phys Rev B 1977;15:4425.
[50] Binder K, Stauffer D. Phys Rev Lett 1974;33(17):1006.